Development of a Post-CMOS Compatible Nanoporous Thin Film layer Based on Al_2O_3

Ö Dogan[1], A Buschhausen[2], C Walk[1], W Mokwa[3] and H Vogt[4]

[1] Fraunhofer Institute for Microelectronic Circuits and Systems, 47057 Duisburg, Germany
[2] Department of Microelectronics, University of Applied Sciences, 40476 Düsseldorf, Germany
[3] Department of Materials in Electrical Engineering 1, RWTH Aachen University, 52074 Aachen, Germany
[4] Department of Electronic Components and Circuits, University of Duisburg-Essen, 47057 Duisburg, Germany
E-mail: oezgue.dogan@ims.fraunhofer.de

Abstract. Porous alumina is a popular material with numerous application fields. A post-CMOS compatible process chain for the fabrication of nanoporous surface based on Al_2O_3 by atomic layer deposition (ALD) is presented. By alternately applying small numbers of ALD cycles for Al_2O_3 and ZnO, a homogenous composite was accomplished, for which the principle of island growth of ALD materials at few deposition cycle numbers was utilised. By selective texture-etching of ZnO content via hydrofluoric acid (HF) in vaporous phase at 40 °C and 10.67 mbar, a porous surface of the etch resistant Al_2O_3 could be achieved. TOF-SIMS investigations verified the composition of ALD composite, whereas AFM and high resolution SEM images characterised the topographies of pre- and post-etched samples. Pores with opening diameters of up to 15 nm could be detected on the surface after vaporous HF treatment for 2 minutes. The amount of pores increased after an etching time of 5 minutes.

1. Introduction

Porous alumina provides numerous applications in several domains of nanotechnology due to its relatively high strength and an improved thermal and chemical stability [1, 2]. It has been established in membrane technology [3 - 5], where pore size and pores amount play a significant role by modulating membrane properties, as a support for heterogeneous catalysts [6, 7] or also as evaporation masks [8]. Especially in the field of medical engineering and biotechnologies porous alumina functions as biocompatible coating for implantable devices, membranes and, especially the porous surfaces, as suitable cell interfaces [9 - 11]. Porous alumina is also well established in the field of resistive or capacitive measurement of relative humidity [12], in which pore size [13] and degree of porosity of the transducing material influence sensor sensitivity significantly by enlarging the surface for interaction with more water molecules [14]. The most common methods for synthetisation of porous Al_2O_3 are annealing at temperatures above 1000 °C [15, 16], anodization in liquid electrolytes [17, 18] or processing by sol-gel method with an additional annealing step [19, 20]. These methods have been well established in the past decades and show sufficient results. Nevertheless, they are aggressive for sensitive substrate materials, may result in inhomogeneous film thickness on complex surfaces and, thus, are not suitable for CMOS post-processing.

In order to avoid the above mentioned disadvantages of synthetisation methods, lower processing temperatures and a more isotropic deposition of the alumina can be applied by using atomic layer deposition (ALD). ALD is a special type of chemical vapour deposition (CVD) processes and ensures a highly conformal and dense thin film coating, even on non-planar, three-dimensional substrate surfaces with high aspect ratios [21]. Additionally, the deposition of Al_2O_3 by an ALD process is possible at temperatures below 300°C [22]. Unlike CVD processes, ALD utilizes an alternating exposure of two precursors. Thus, the substrate surface can be saturated with respective chemicals in each deposition cycle, so that film growth is self-limiting. This enables well-controlled film growth, with a specific growth rate, and layer thicknesses.
Based on mentioned properties of ALD layers; production of porous ALD ceramics cannot be implemented without additional process steps. A known method for generating porosity in an ALD layer is the deposition of a hybrid material by alternately applying an organic and inorganic precursor in terms of a molecular layer deposition (MLD). By post-deposition annealing or wet-etching procedures, the organic part of the ALD/MLD material can be removed so that a porous, inorganic oxide backbone is left [23, 24]. Nevertheless, the reproducibility of ALD processes is more manageable than MLD processes [25]. This is why inorganic precursors are considered in this paper, only. ALD of ceramics are well tested and established processes. Especially the deposition of Al_2O_3 with trimethylaluminum and water ($AlME_3/H_2O$) can be considered as the most typical and studied ALD process.
Therefore, a composite of Al_2O_3 and ZnO by ALD has been developed which shall be textured by treatment with vaporous hydrofluoric acid (vHF). Regarding [26, 27], a selective etching of the ZnO grain boundaries is expected, whereas the etch-resistant Al_2O_3 content shall remain. Furthermore, etching could occur at weak chemical bonds between Al_2O_3 and ZnO grain boundaries. Both mechanisms would lead to texturing of the composite and, thus, to a nanoporous composite layer (see figure 1).

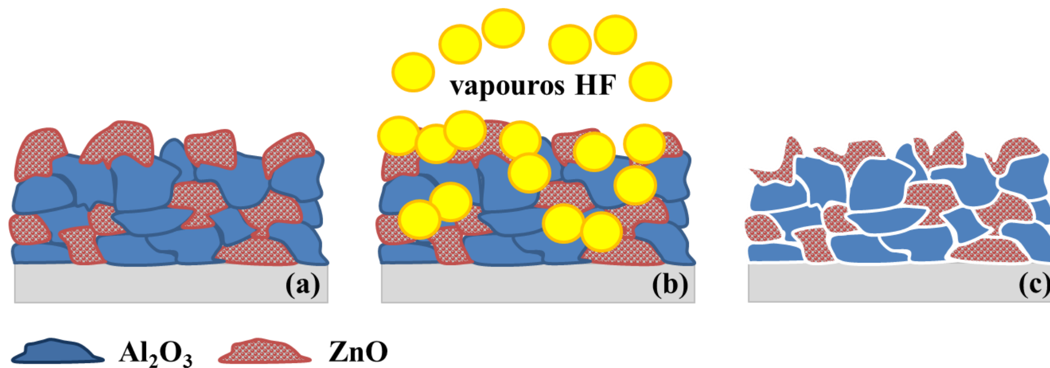

Figure 1. Schematic view of fabrication process of a nanoporous composite layer by ALD. (a) Al_2O_3-ZnO composite, (b) exposure to vaporous HF, (c) resulting nanoporous composite layer.

For a homogenous composite of both oxides, the principle of island growth at small numbers of deposition cycles has been utilised. If the growth of a metal oxide is substrate-inhibited, growth rate in the first deposition cycles can be much smaller than growth rates on ALD grown materials. Considering steric hindrances from precursor molecules and localised distribution of active sites on the substrate surface, island growth of respective materials can be achieved, if the amount of deposition cycles is small enough to prevent touching of neighbouring islands, which continuously grow with each additional deposition cycle [28].
In this paper, three ALD recipes have been investigated with TOF-SIMS to find a homogeneous Al_2O_3-ZnO composite. Most promising layers have been etched in vHF. AFM measurement and high-resolution SEM pictures compare pre- and post-etched results to verify the best route to fabricate a nanoporous surface.

2. Experimental details

In this work, three Al_2O_3-ZnO composite depositions were accomplished on silicon substrates with a thermal ALD equipment type “R200” from “Picosun Oy” which is a single-wafer reactor with vertical gas flow. Nitrogen (N_2) was used as carrier and purging gas. The deposition temperature was 270 °C. According to [28], Al_2O_3 islands grow starts at active defects within the substrate surface during the first ALD cycle. Islands grow laterally with each additional deposition cycles and start to touch each other after a certain number of cycles. Thus, island coalescence begins and results into a continuous film, if this certain cycle number is exceeded. Since this number is 16 in [28], smaller numbers of deposition cycles were chosen in this work. Used precursors were trimethylaluminum ($AlME_3$) and water (H_2O) for Al_2O_3 and diethylzinc (DEZ) and H_2O for ZnO. Every composite film was deposited using 0.1 s $AlME_3$ and 0.1 s H_2O pulses for Al_2O_3 with 6 s and 10 s purging steps, respectively. ZnO was deposited using 0.1 s DEZ and 0.2 s H_2O pulses with purging times of 6 s and 10 s. In order to define the upper limit of cycle numbers for a homogenous composition instead of a nanolaminate, different cycle numbers (*x* for alumina, *y* for zinc oxide) and oxide ratios were applied. One deposition period of Al_2O_3 first and ZnO second was defined as one super-cycle. Detailed process parameters are listed in table 1.

Table 1. Deposition cycle numbers, mixture ratio and super cycle numbers.

Sample #	*x*	*y*	Ratio *x*:*y*	Super cycle
1	8	8	1.00	35
2	12	10	1.20	25
3	15	12	1.25	21

Distribution of different oxide clusters within the composite was investigated by time-of-flight secondary ion mass spectrometry (“TOF.SIMS^5-100” from “ION-TOF” GmbH) which allows depth profiling with resolutions of < 1 nm per sputter step. An area of 10000 µm² was monitored and an average of intensity was calculated for detected fragments. Intensity trends with respect to sputter depth reveal information about the composition of Al_2O_3 and ZnO in the deposited ALD composites.
The isotropic and selective texture-etching of the composite contents via vHF is performed in the "Sacrificial Layer Release System" from "memsstar". This system comprises load lock, transfer module and process modules, of which one is capable of applying gaseous hydrofluoric acid (HF). In this process module, the pressure is controlled by the opening angle of the valve on the tube to the vacuum pump. For first experiments, the temperature, the pressure and total gas flows were hold constant at 40 °C. Higher pressures or lower process temperatures promote the condensation of water vapour. Thus, the catalytic effect of liquid water and total etching process is promoted as well [29]. Before the as described depositions were treated with HF in vapour phase (HF concentration 40 %), the texture-etching for ALD deposited ZnO was successfully tested at 10.67 mbar. On the contrary, Al_2O_3 did not exhibit any indications for successful etching at the same process pressure. ALD composite samples were treated with vHF for 2 and 5 minutes at 40 °C process temperature and 10.67 mbar process pressure.
Roughness of etched and not etched samples are compared by atomic force microscope (AFM) measurements (“D5000V” from “Veeco”) recorded in taping mode. Scanning electron microscope (SEM) images of sample topographies were recorded with ultra-high resolution field emission SEM (“JSM-7500F” from “JEOL”).

3. Results and discussion

3.1. TOF-SIMS

Composition of Al_2O_3 and ZnO contents is investigated by TOF-SIMS. Measured intensity signals of detected Al_2O_3 and ZnO fragments are presented in figure 2 – 5. As shown in figure 2, intensities of composite materials of sample 1 significantly decrease at the interface to the bulk material, where the

intensity of detected bulk silicon increases at the same sputter depth. Figure 3 shows the enlarged depth within the range of ALD composite thickness (100 nm). Intensities of Al_2O_3 and ZnO are constant which results into a constant ratio, as well. This indicates that the amount of Al_2O_3 and ZnO clusters are constant at every sputter step through the whole oxide composite.

As shown in figure 4, the interface between ALD composite and bulk material of sample 3 is at about 166 nm. Detected intensities are obviously alternating during the whole sputter depth, which can be seen in the magnified range of composite thickness (figure 5). Based on period lengths of phase shifted intensities, a nanolaminate (or at least layers with significant predominant content of single materials) with Al_2O_3 layers of up to 5 nm thickness and ZnO layers of up to 3 nm thickness is extracted. SIMS results of sample 2 also showed phase-shifted intensities of Al_2O_3 and ZnO with smaller period lengths, which indicate thinner laminate-layers (approx. 2 nm). Since the intensity trends are very similar to the intensity trends of sample 3, they are not presented additionally.

Composites with 12 and 10 or 15 and 12 deposition cycles for Al_2O_3 and ZnO, respectively, showed nanolaminate properties. A vHF treatment would only lead to a texture-etching at the grain boundaries of the top ZnO film, whereas the underlying alumina film serves as an etch stop. Thus, a required porosity might not be achieved. Therefore, sample 2 and 3 are not further considered for etching steps and characterisations. Sample 1 showed continuously unchanged intensity signals over the whole ALD composite film which means that 8 deposition cycles of Al_2O_3 and ZnO, each, are suitable for achievement of island growth.

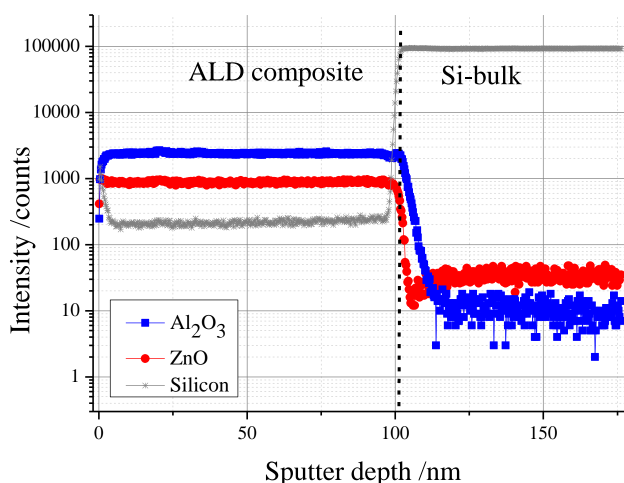

Figure 2. Sample 1 with each 8 deposition cycles, composite-bulk interface at 100 nm.

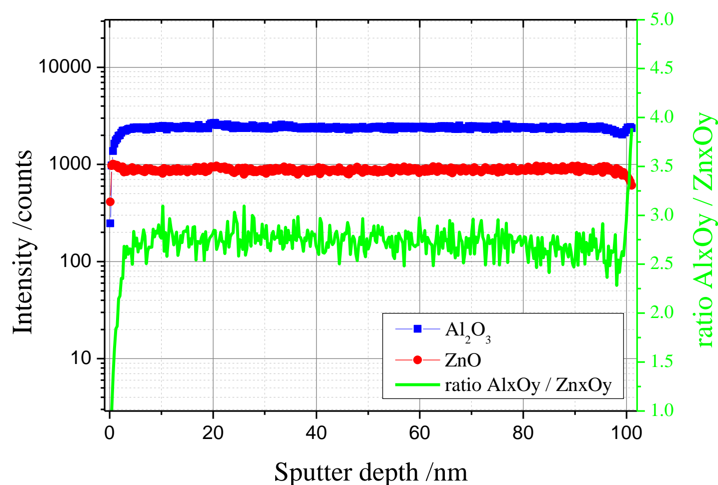

Figure 3. Sample 1 - magnified area with unchanged intensities of Al_2O_3 / ZnO and constant ratio thereof.

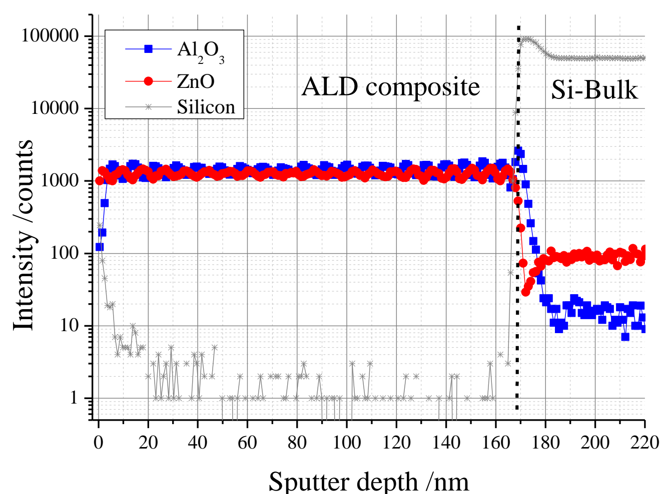

Figure 4. Sample 3 with 15 cycles Al_2O_3 and 12 cycles ZnO, composite-bulk interface at about 166 nm.

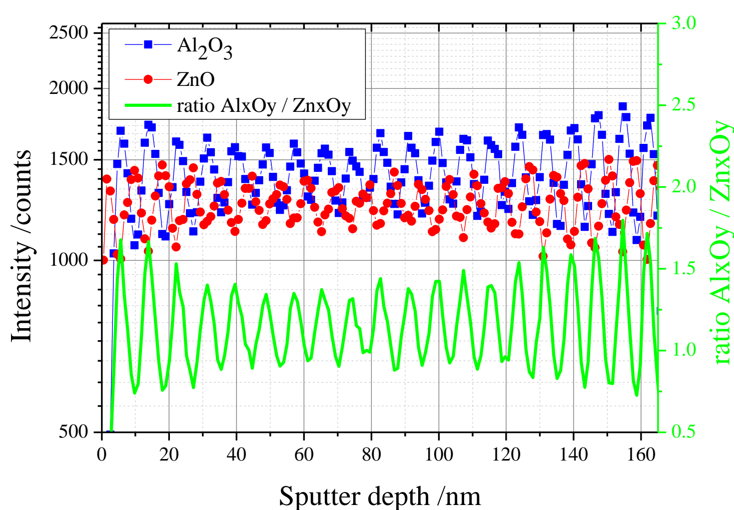

Figure 5. Sample 3 – magnified area with continuously phase-shifted intensities of Al_2O_3 / ZnO and alternating ratio.

3.2. AFM

AFM measurements were accomplished at tapping mode with a velocity of 0.3 µm per second and 256 measured lines (256 measurement points per line). Hill-like elevations of up to 6 nm were measured due to alternately applied ALD of two oxides and their different growth rate and behaviour. Figure 6 (a) presents the topography of the not etched ALD composite. Measured roughness was 1.15. This value is comparable with a roughness of 1.08 of the composite which was etched by vHF for 5 minutes (shown in figure 6 (b)). Even though roughness results are very similar, differences in granularity are obvious. The not etched sample showed a smaller granularity whereas the etched sample revealed bigger grain sizes. A reason for smaller grain sizes for the as-deposited composite is different growth behaviours of Al_2O_3 and ZnO. Both oxides have various growth rates as well on foreign substrate materials as on same ALD-grown materials. A mixture of both oxides with few deposition cycles leads to a composite with a granular topography due to continuous island growth while an increased number of deposition cycles allows the current material to grow more conformal.

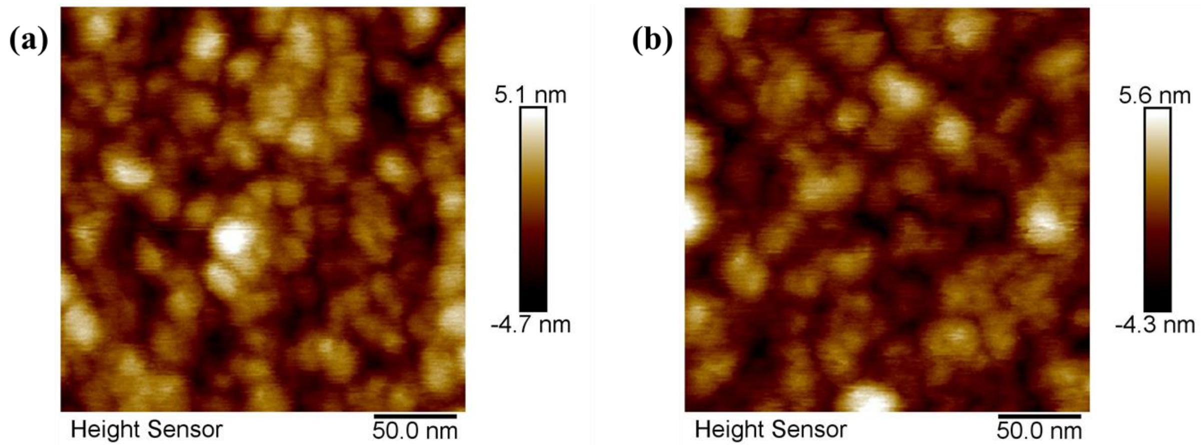

Figure 6. Topographies as measured by AFM of sample 1 (a) before etching and (b) after etching with vHF for 5 minutes at 10.67 mbar and 20 °C.

AFM images of sample 2 and 3 showed the same trend in granularity on the composite surface. The bigger the number of deposition cycles the bigger the hill-like elevations on the sample's surface. By applying vHF, the surface was texture-etched and the granularity seemed to increase. Porosity cannot be determined with the images of figure 6, since AFM cannot reveal information about a deepening, whose inner diameter is bigger than the opening diameter.

3.3. Ultra-High Resolution SEM

Uneven surfaces of not etched samples can be seen on high-resolution SEM images with a magnification factor of 200 k (figure 7). Granular surface of the untreated ALD composite can be seen on figure 7 (a), whereas (b) and (c) show vHF treated composites after 2 minutes and 5 minutes of etching, respectively. Already after 2 minutes (the shortest etching time used) pores could be seen. The number of pores seems to increase with increased etching time. Measured pore diameters varied from approximately 3 nm to 15 nm for 2 minutes and 5 minutes etched composites.

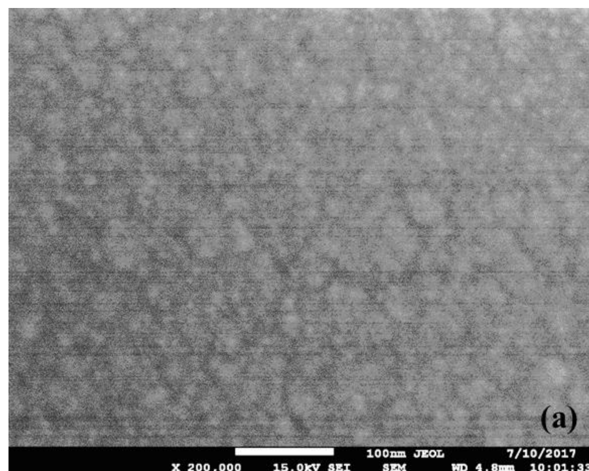

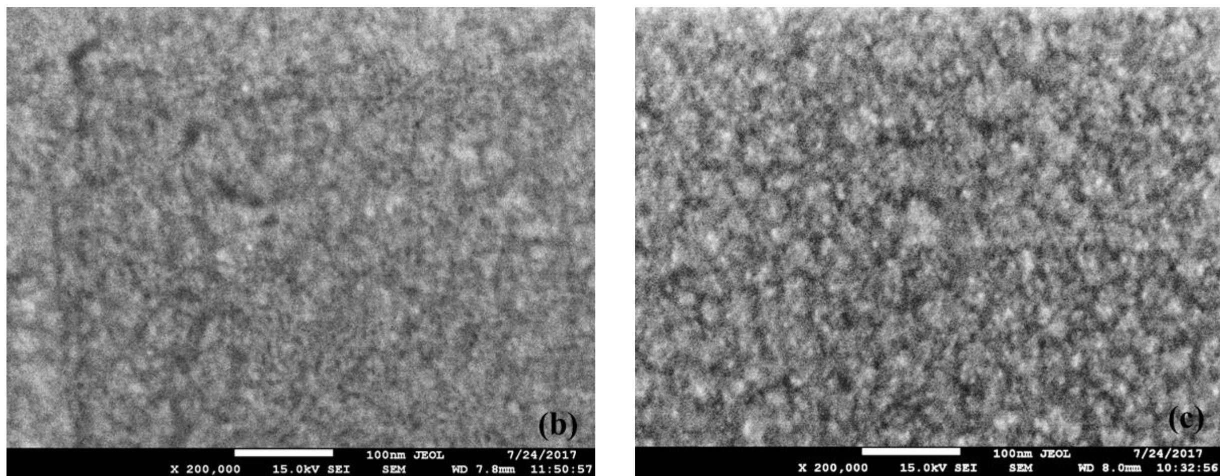

Figure 7. SEM images with magnification factor 200 k of (a) sample 1 (b) sample 1 after vHF treatment for 2 minutes and (c) sample 1 after vHF treatment for 5 minutes.

4. Summary and conclusion

Preliminary experiments verified a novel process for fabrication of porous ALD thin film layer based on alumina, which is deposited by a special ALD process, in this work. To reach this, a homogenous ALD composite with Al_2O_3 and ZnO was needed. By TOF-SIMS investigations of three different ALD recipes with various deposition cycle numbers, an upper limit of deposition cycle number could be defined for prevention of a nanolaminate. By applying 8 cycles of Al_2O_3 and 8 cycles of ZnO alternately, only island growth could be achieved, so that selective texture-etching of the ZnO content could lead to porosity on the surface of the ALD composite. Granularity and roughness were compared by AFM results. Even though roughness didn't change after vHF treatment, grain sizes on the etched surface seem to increase after texture-etching. High-resolution SEM images showed topographies of pre- and post-etched composites. Pores with diameters of up to 15 nm could be detected after a vHF treatment of 2 minutes. By applying a longer etching time, the amount of pores on the surface of the composite increased.

This work shows a process chain with only two fabrication steps for the development of a porous thin film layer which is based on alumina. Considering the application of humidity measurement, pores with diameters of approximately 2 - 10 nm are desired for detection of low relative humidity values since they promote trapping of gaseous water molecules (of the same size) more effectively [13]. Pores with diameters up to 15 nm could be processed by vHF treatment of an ALD composite with, alternately applied, 8 deposition cycles for each Al_2O_3 and ZnO. The amount of pores on the surface of the composite could be increased by increasing the etching time. As future work, the tailoring of pore size and degree of porosity of vHF treated ALD composites with smaller numbers of Al_2O_3 and ZnO deposition cycles and ratios, and various etching times will be investigated. It is assumed that a customised porous layer based on Al_2O_3 could be fabricated for humidity measurement, for example.

The presented process steps are compatible to CMOS by fulfilling temperature limits and choice of materials. The etching medium vHF can be applied as well if an appropriate etching barrier layer is used in order to protect the CMOS substrate [30]. Thus, this process chain is suitable for post-processing of all kind of CMOS chips.

5. References

[1] Poco J F, Satcher Jr. J H and Hrubesh L W 2001 Synthesis of high porosity, monolithic alumina aerogels *Journal of Non-Crystalline Solids* vol 285 pp 57-63

[2] Eklund P, Sridharan M, Singh G, Bottiger J 2009 Thermal Stability and Phase Transformations of γ-/Amorphous-Al_2O_3 Thin Films *Plasma Processes and Polymers* vol 6 pp 5907-5911

[3] Hsieh H P, Liu P K T and Dillman T R 1991 Microporous Ceramic Membranes *Polymer Journals* vol 23 (5) pp 407-415

[4] Sola L, Alvarez J, Cretich M, Swann M J, Chiari M, Hill D 2015 Characterization of porous alumina membranes for efficient, real-time, flow through biosensing *Journal of Membrane Science* vol 476 pp 128-135
[5] Bocchetta P, Chiavarotti G P, Di Q F, Gullo U, Sunseri C 2004 Process for manufacturing a porous alumina membrane for fuel cells, EP1391235 A2
[6] Patermarakis G and Pavlidou C 1994 Catalysis over Porous Anodic Alumina Catalysts *Journal of Catalysis* vol 147 pp 140-155
[7] Zapf R et al. 2003 Detailed characterization of various porous alumina-based catalyst coatings within microchannels and their testing for methanol steam reforming *Chemical Engineering Research and Design* vol 81 pp 721-729
[8] Masuda H and Satoh M 1996 Fabrication of Gold Nanodot Array Using Anodic Porous Alumina as an Evaporation Mask Japanese Journal of Applied Physics vol 35 (2) pp 126-129
[9] Gultepe E, Nagesha D, Sridhar S and Amiji M 2010 Nanoporous inorganic membranes or coatings for sustained drug delivery in implantable devices *Advanced Drug Delivery Reviews* vol 62 Issue 3 pp 305-315
[10] Brüggemann D 2013 Nanoporous Aluminum Oxide Membranes as Cell Interfaces *Journal of Nanomaterials* Article ID 460870
[11] La Flamme K E, Popat K C, Leonie L, Markiewicz E, La Tempa T J, Roman B B, Grimes C A, Desai T A 2007 Biocompatibility of nanoporous alumina membranes for immunoisolation *Biometarials* vol 28 pp 2638-2645
[12] Khanna V K and Naher R K 1986 Carrier-transfer mechanisms and Al_2O_3 sensors for low and high humidities *Journal of Physics D: Applied Physics* vol 19 pp 141-145
[13] Connolly E J, French P J, Pham H T M and Sarro P M 2002 Relative Humidity Sensors Based on Porous Polysilicon and Porous Silicon Carbide *IEEE Sensors* vol 1 pp 499-502
[14] Chou K-S, Lee T-K and Liu F-J 1999 Sensing mechanism of a porous ceramic as humidity sensor *Sensors and Actuators B* vol 56 pp 106-111
[15] Wang H A and Kröger F A 1989 Pore formation during oxidative annealing of Al_20_3- : Fe and slowing of grain growth by precipitates and pores *Journal of Material Science* vol 15 Issue 8 pp 1978–1986
[16] Furlan K P, Pasquarelli R M, Krekeler T, Ritter M, Zierold R, Nielsch K, Schneider G A and Janssen R 2017 Highly porous α-Al2O3 ceramics obtained by sintering atomic layer deposited inverse opals *Ceramics International* vol 43 pp 11260-11264
[17] Smith A 1974 Process for producing an anodic aluminum oxide membrane, US 3850762 A
[18] Chen Z, Jin M-C, Zhen C and Chen G-H 1991 Properties of Modified Anodic-Spark-Deposited Alumina Porous Ceramic Films as Humidity Sensors *Journal of the American Ceramic Society* vol 74 (6) pp 1325-1330
[19] Bagwell R B and Messing G L 1996 Critical Factors in the Production of Sol-Gel Derived Porous Alumina *Key Engineering Materials* vol 115 pp 45-64
[20] Farahmandjou M and Golabiyan N 2015 New pore structure of nano-alumina (Al_2O_3) prepared by sol gel method *Journal of Ceramic Processing Research* vol 16 (2) pp 1-4
[21] Ritala M and Niinistö J 2009 *Chemical Vapour Deposition: Precursors, Processes and Applications* vol 1, ed A C Jones and M L Hitchman pp 158-206
[22] Puurunen R L 2005 Surface chemistry of atomic layer deposition: A case study for the trimethylaluminum/water process *Journal of Applied Physics* vol 97 Article ID 121301
[23] Sundberg P and Karppinen M 2014 Organic and inorganic-organic thin film structures by molecular layer deposition: A review *Beilstein Journal of Nanotechnology* vol 5 pp 1104-1136
[24] Lausund K B and Nilsen O 2016 All-gas-phase synthesis of UiO-66 through modulated atomic layer deposition *Nature Communications* vol 7 Article ID 13578
[25] George S M, Yoon B and Dameron A A 2009 Surface Chemistry of Molecular Layer Deposition of Organic and Hybrid Organic-Inorganic Polymers *Accounts of Chemical Research* vol 42 (4) pp 498-508

[26] Hüpkes J, Zhu H, Owen J I, Jost G and Bunte E 2012 Instabilities in reactive sputtering of ZnO:Al and reliable texture-etching solution for light trapping in silicon thin film solar cells *Thin Solid Films* vol 520 pp 1913-1917
[27] Lee Y-J, Park H, Ju M, Kim Y, Park J, Ai D V, Hussain S Q, Lee Y, Ahn S and Yi J 2014 Improvement of haze ratio of DC (direct-current)-sputtered ZnO:Al thin films through HF (hydrofluoric acid) vapor texturing *Energy* vol 66 pp 20-24
[28] Puurunen R L and Vandervorst W 2004 Island growth as a growth mode in atomic layer deposition: A phenomenological model *Journal of Applied Physics* vol 96 pp 7686-7695
[29] Drysdale D, O'hara T and Wang C H 2011 Characterisation and comparison of water and alcohol as catalysts in vapour phase HF etching of silicon oxide films *Symposium on Design, Test, Integration Packaging of MEMS/MOEMS (DTIP)* pp 35-40
[30] Walk C, Chen Y, Vidovic N, Kuhl A, Görtz M and Vogt H 2016 Development of a low temperature SiC protection layer for post-CMOS MEMS fabrication utilizing vapour release technologies *Micro-Nano-Integration (6. GMM-Workshop)* pp 126-131